Deriving confidence intervals for mutation rates across a wide range of evolutionary distances using FracMinHash

Mahmudur Rahman Hera, N. Tessa Pierce-Ward and David Koslicki

Genome Res. published online June 21, 2023
Access the most recent version at doi:10.1101/gr.277651.123

Deriving confidence intervals for mutation rates across a wide range of evolutionary distances using FracMinHash

Mahmudur Rahman Hera[1], N. Tessa Pierce-Ward[2], and David Koslicki[1,3,4,‡]

[1] Department of Computer Science and Engineering, The Pennsylvania State University
[2] Department of Population Health and Reproduction, University of California, Davis
[3] Department of Biology, The Pennsylvania State University
[4] Huck Institutes of the Life Sciences, The Pennsylvania State University
‡ Corresponding author, dmk333@psu.edu

Abstract. Sketching methods offer computational biologists scalable techniques to analyze data sets that continue to grow in size. MinHash is one such technique to estimate set similarity that has enjoyed recent broad application. However, traditional MinHash has previously been shown to perform poorly when applied to sets of very dissimilar sizes. *FracMinHash* was recently introduced as a modification of MinHash to compensate for this lack of performance when set sizes differ. This approach has been successfully applied to metagenomic taxonomic profiling in the widely used tool `sourmash gather`. While experimental evidence has been encouraging, FracMinHash has not yet been analyzed from a theoretical perspective. In this paper, we perform such an analysis to derive various statistics of FracMinHash, and prove that while FracMinHash is not unbiased (in the sense that its expected value is not equal to the quantity it attempts to estimate), this bias is easily corrected for both the containment and Jaccard index versions. Next, we show how FracMinHash can be used to compute point estimates as well as confidence intervals for evolutionary mutation distance between a pair of sequences by assuming a simple mutation model. We also investigate edge cases where these analyses may fail, to effectively warn the users of FracMinHash indicating the likelihood of such cases. Our analyses show that FracMinHash estimates the containment of a genome in a large metagenome more accurately and more precisely when compared to traditional MinHash, and the point estimates and confidence intervals perform significantly better in estimating mutation distances.

Introduction

One strategy scientists use when analyzing large data sets is to create a low-dimensional "sketch" or "fingerprint" of their data that allows fast, but approximate answers to their query of interest. Such sketching-based approaches in recent years have been successfully applied to a variety of genomic and metagenomic analysis tasks, due in large part to such methods incurring low computational burden when applied to large data sets. For example, Mash (Ondov et al 2016), is a MinHash (Broder 1997)-based approach that was used to characterize the similarity between all pairs of RefSeq genomes in less than 30 CPU hours. Such efficiency gains are due primarily to sketching-based approaches recording a small subsample (or modification thereof) of the data in such a fashion that some distance metric or similarity measure is approximately preserved, a process called a locality sensitive hashing scheme. In bioinformatics, this has resulted in improvements to error correction (Miclotte et al 2015; Sahlin and Medvedev 2021), assembly (Birol et al 2009; Chin and Khalak 2019; Ekim et al 2021; Ghosh and Kalyanaraman 2017), alignment (Jain et al 2018; Li 2018), clustering (Crusoe et al 2015; Koslicki and Zabeti 2019; Pierce et al 2019; Zhang et al 2014), classification (Breitwieser et al 2018; LaPierre, Alser, et al 2020; LaPierre, Mangul, et al 2019), and so on. Importantly, the accuracy and efficiency of sketching approaches can frequently be characterized explicitly, allowing practitioners to balance between efficiency improvements and accuracy. Often, these theoretical guarantees dictate that certain sketching approaches are well suited only to certain kinds of data. For example, MinHash, which is used in many of the aforementioned applications, has been shown to be particularly well-suited to quantify the similarity of sets of roughly the same size, but falters when sets of very different sizes are compared (Koslicki and Zabeti 2019). This motivated the introduction of the containment MinHash which utilized a MinHash sketch of the smaller set, with an additional probabilistic data structure (a Bloom filter (Bloom 1970)) to store the larger set. While this improved speed and accuracy, this approach can become quite inconvenient for large sets due to requiring a bloom filter to be created for the larger of the two sets.

To ameliorate this, an approach called the "FracMinHash" was recently introduced (Irber et al 2022; Irber Jr 2020) that uses a MinHash hash selection approach but allows sketch size to scale naturally with the size of the underlying data, similar to ModHash dynamic scaling (Broder 1997). These properties allow both Jaccard and containment estimation between FracMinHash sketches, extending the computational advantages of MinHash sketches beyond similar-sized genome comparisons to sequencing datasets of all types. Most notably, FracMinHash enables large-scale metagenome analyses, including genomic and metagenomic similarity assessment, metagenomic taxonomic classification, streaming database searches, and outbreak detection via genomic surveillance (Pierce et al 2019; Viehweger et al 2021). FracMinHash sketching is implemented in a software package called sourmash (Brown and Irber 2016). Independently, and more recently, the same concept of FracMinHash was introduced with the name *universe minimizer* (Ekim et al 2021).

While there is ample computational evidence for the superiority of FracMinHash when compared to the classic MinHash, particularly when comparing sets of different sizes, no theoretical characterization about the accuracy and efficiency of the FracMinHash approach has yet been given. In this manuscript, we address this missing characterization of accuracy and efficiency by deriving a number of theoretical guarantees. In particular, we demonstrate that the FracMinHash approach, as originally introduced, requires a slight modification in order to become an unbiased estimator of the containment index (in terms of expected value). After this, we characterize the statistics of this unbiased estimator and derive an asymptotic normality result for FracMinHash. This in turn allows us to derive confidence intervals and hypothesis tests for this estimator when considering a simple mutation model (which is related to the commonly used Average Nucleotide Identity (ANI) score). We also characterize the likelihood of experiencing an edge case when analyzing real

data which allows us to provide a level of confidence along with the estimated containment index. Finally, we support the theoretical results with additional experimental evidence and compare our approach to the frequently used Mash distance (Ondov et al 2016). Many of these theoretical findings have already been implemented into the sourmash (Brown and Irber 2016) computational package (see https://github.com/sourmash-bio/sourmash/pull/1967 and https://github.com/sourmash-bio/sourmash/pull/2032). A Python-based implementation of the theorems we derive is freely available at https://github.com/KoslickiLab/mutation-rate-ci-calculator. An extended version of this manuscript is available here: https://doi.org/10.1101/2022.01.11.475870.

Methods

In this section, we describe theoretical analyses of the containment index using FracMinHash. For the sake of continuity from a reader's perspective, we have included proofs of all theorems in the supplemental materials (Section A.3).

FracMinHash and its statistics

We begin by formally defining a FracMinHash sketch by slightly modifying the definition in (Irber et al 2022). We aim to compare two sequences by computing the containment index from their corresponding FracMinHash sketches.

Definitions and preliminaries We recall the definition of FracMinHash given in (Irber et al 2022). Given two arbitrary sets A and B which are subsets of a domain Ω, the containment index $C(A,B)$ is defined as $C(A,B) := \frac{|A\cap B|}{|A|}$. Let h be a perfect hash function $h : \Omega \to [0,H]$ for some $H \in \mathbb{R}$. For a *scale factor* s where $0 \leq s \leq 1$, a FracMinHash sketch of a set A is defined as follows:

$$\mathbf{FRAC}_s(A) = \{\, h(a) \mid a \in A \text{ and } h(a) \leq Hs \}\,. \tag{1}$$

The scale factor s is an easily tunable parameter that can modify the size of the sketch. Using this FracMinHash sketch, we define the FracMinHash estimate of the containment index $\hat{C}_{\text{frac}}(A,B)$ as follows:

$$\hat{C}_{\text{frac}}(A,B) := \frac{|\mathbf{FRAC}_s(A) \cap \mathbf{FRAC}_s(B)|}{|\mathbf{FRAC}_s(A)|}. \tag{2}$$

Simply speaking, we want to compute $\hat{C}_{\text{frac}}(A,B)$ because the sketches are considerably smaller than the original sets A and B, and we want $\hat{C}_{\text{frac}}(A,B)$ to accurately approximate $C(A,B)$.

For notational simplicity, let us define $X_A := |\mathbf{FRAC}_s(A)|$. We observe that if one views h as a uniformly distributed random variable, we have that X_A is distributed as a binomial random variable: $X_A \sim \text{Binom}(|A|, s)$. In practice, hashing libraries use large enough hash value space (i.e. 2^{64}) and well enough hash functions that the assumptions on h are mostly valid. Furthermore, if $A \cap B \neq \emptyset$ where both A and B are non-empty sets and one is not a subset of the other, then $X_{A\setminus B}$ and $X_{A\cap B}$ are independent when the probability of success, s, is strictly smaller than 1. Using these notations, the expectation of $\hat{C}_{\text{frac}}(A,B)$ is given by Theorem 1, recapitulated from (Irber et al 2022) for completeness.

Theorem 1. *For $0 < s < 1$, if A and B are two non-empty sets such that $A \setminus B$ and $A \cap B$ are non-empty, the following holds:*

$$\mathrm{E}\left[\hat{C}_{frac}(A,B)\mathbb{1}_{|\mathbf{FRAC}_s(A)|>0}\right] = \frac{|A\cap B|}{|A|}\left(1-(1-s)^{|A|}\right).$$

In light of Theorem 1, we note that $\hat{C}_{\text{frac}}(A,B)$ is *not* an unbiased estimate of $C(A,B)$: the expected value of $\hat{C}_{\text{frac}}(A,B)$ is not equal to $C(A,B)$. This may explain the observations in (Irber Jr 2020) that showed the uncorrected version in eq. (2) leads to suboptimal performance for short sequences (e.g viruses). However, for sufficiently large $|A|$ and s, the bias factor $\left(1-(1-s)^{|A|}\right)$ is sufficiently close to 1. Alternatively, if $|A|$ is known (or estimated, eg. by using HyperLogLog (Flajolet et al 2007) or the estimate in Section A.6), then

$$C_{\text{frac}}(A,B) := \frac{|\mathbf{FRAC}_s(A) \cap \mathbf{FRAC}_s(B)|}{|\mathbf{FRAC}_s(A)|\left(1-(1-s)^{|A|}\right)} \mathbb{1}_{|\mathbf{FRAC}_s(A)|>0} \tag{3}$$

is an unbiased estimate of the containment index $C(A,B)$. Throughout the rest of the paper, we will refer to the debiased $C_{\text{frac}}(A,B)$ as the *fractional containment index*.

Mean and variance of $C_{\text{frac}}(A,B)$ The expectation of $C_{\text{frac}}(A,B)$ is as follows.

Theorem 2. *For $0 < s < 1$, if A and B are two distinct sets such that $A \setminus B$ and $A \cap B$ are non-empty, the expectation of $C_{frac}(A,B)$ is given by*

$$\mathrm{E}[C_{frac}(A,B)] = \frac{|A \cap B|}{|A|}. \tag{4}$$

Proof. This follows directly from Equation (3) and Theorem 1. ■

We now turn to determining the variance of $C_{\text{frac}}(A,B)$. Ideally, we can do so by using the multivariate probability mass function of $X_{A\cap B}$ and $X_{A\setminus B}$. However, we found that doing so does not result in a closed-form formula. Therefore, we use Taylor expansions to approximate the variance.

Theorem 3. *For $n = |A \cap B|$ and $m = |A \setminus B|$ where both m and n are non-zero, a first order Taylor series approximation gives*

$$\mathrm{Var}\left[\hat{C}_{frac}(A,B)\right] \approx \frac{mn(1-s)}{s(m+n)^3}.$$

Using the results of Theorem 3 and Equation (3), we have the variance of $C_{\text{frac}}(A,B)$ as follows.

Corollary 1. *For $n = |A \cap B|$ and $m = |A \setminus B|$ where both m and n are non-zero, a first order Taylor series approximation gives*

$$\mathrm{Var}\left[C_{frac}(A,B)\right] \approx \frac{mn(1-s)}{s(m+n)^3\left(1-(1-s)^{|A|}\right)^2}.$$

Proceeding in the same fashion, we can obtain series approximations of arbitrarily high order due to the binomial distribution having finite central moments of arbitrary order. However, we found that the higher order expansion derivations are tedious and long, whereas the results obtained using first order approximation are both simple and accurate enough in practice.

Asymptotic normality of $C_{\text{frac}}(A,B)$ We next prove that $C_{\text{frac}}(A,B)$ is asymptotically normal. We utilize the delta method (Agresti 2012) combined with the De Moivre-Laplace theorem, which guarantees asymptotic normality of $X_{A\cap B}$ and $X_{A\setminus B}$, and since $g(x,y) = \frac{x}{x+y}$ is a function that is twice differentiable, setting $x = X_{A\cap B}$ and $y = X_{A\setminus B}$ satisfies all requirements of using the delta method on $g(x,y)$, which gives us the following result:

Theorem 4. *For $g(x,y) = \frac{x}{x+y}$, $n = |A \cap B|$ and $m = |A \setminus B|$ where both m and n are non-zero,*

$$\sqrt{n+m}\left(g(X_{A\cap B}, X_{A\setminus B}) - g(n,m)\right) \xrightarrow[n,m\to\infty]{\mathscr{D}} \mathcal{N}\left(0, \frac{mn(1-s)}{(m+n)^3 s}\right).$$

We note that additional statistical quantities can easily be derived. For example, in Section A.5 we provide concentration inequalities that demonstrate theoretically how little $C_{\text{frac}}(A,B)$ deviates from its expected value. Section A.6 provides a simple way to calculate the number of distinct k-mers from a given sketch. Lastly, Section A.7 demonstrates how to compute (and de-bias) a Jaccard estimate from FracMinHash sketches.

Statistics of $C_{\text{frac}}(A,B)$ under simple mutation model

In the previous section, we introduced $C_{\text{frac}}(A,B)$, and derived its statistics. In this section, we use these results and connect $C_{\text{frac}}(A,B)$ to a biologically meaningful quantity – the Average Nucleotide Identity (ANI) and mutation rate. We do this by assuming a simple mutation model, where each nucleotide of some sequence S is independently mutated at a fixed rate, p, resulting in the mutated sequence S' which has expected ANI of $1-p$ with S. This model was recently introduced in (Blanca et al 2022) where it was quantified how this mutation process affects the k-mers in S.

Before mentioning the details of the mutation model, it is important to note that there are other models of evolution, e.g. TK4 and TK5 models (Takahata and Kimura 1981), the general time reversible (GTR) model (Tavaré 1984) and Sueoka's model (Sueoka 1995). These vary in the number of parameters used, as well as the degree of complexity. In this work, we consider the simple mutation model because (a) the statistics of k-mers under this model are already well explored, and (b) it allows us to connect $C_{\text{frac}}(A,B)$ and mutation rate p directly, which would not be the case if we considered one of these more nuanced models. The mutation model we use, even though simple enough to be mathematically tractable, is more realistic that the Poisson model assumed by Mash (Ondov et al 2016), which assumes that all k-mers are mutated independently, where in reality, one point mutation can affect up to k number of k-mers. Our experiments reveal that even in case of real genomes, where the lengths of two sequences can be widely dissimilar and clearly the assumptions of the simple mutation model are violated, our approach can accurately determine the mutation rate (and ANI) between two real-world sequences.

Preliminaries Here, we closely follow the exposition contained in (Blanca et al 2022). Let $L > 0$ be a natural number that denotes the number of k-mers in some string S. A *k-span* K_i is the range of integers $[i, i+k-1]$ which denotes the set of indices of the sequence S where a k-mer resides. Fix a *mutation rate* p where $0 < p < 1$. The *simple mutation model* considers each position in $i = 1, \ldots, L+k-1$ and with probability p, marks it as *mutated*. A mutation at location i *affects* the k-spans $K_{\max(1,i-k+1)}, \ldots, K_i$. Let N_{mut} be a random variable defined to be the number of affected/mutated k-spans. We use $q = 1-(1-p)^k$ to express the probability that a k-span is mutated. Note that $1-p$ corresponds precisely to the expected average nucleotide identity (ANI) between a sequence S and its mutated counterpart S'.

Given a nonempty sequence S on the alphabet $\{A,C,T,G\}$ and a k-mer size such that each k-mer in S is unique, let A represent the set of all k-mers in S and let $L = |S| - k + 1$. Now, we apply the simple mutation model to S via the following: if for any $i \in [1, \ldots, L+k-1]$, this index is marked as mutated, let ${S'}_i$ be some nucleotide in $\{A,C,T,G\} \setminus \{S_i\}$, and otherwise let ${S'}_i = S_i$. Let B represent the set of k-mers of S', and we assume that S' does not contain repeated k-mers either. In summary, A denotes the set of k-mers of a sequence S, and B denotes the set of k-mers of

a sequence S' derived from S using the simple mutation model with no spurious matches. Note that given a sufficiently large k-mer size, these assumptions will be satisfied in most practical scenarios.

We also recall the definition of a confidence interval. Given a distribution and a parameter of interest τ, a $(1-\alpha)$-CI is an interval that contains τ with probability $1-\alpha$. Given $0 < \alpha < 1$, we define $z_\alpha = \Phi^{-1}(1-\alpha/2)$, where Φ^{-1} is the inverse CDF of the standard Gaussian distribution.

Expectation and variance of $C_{\text{frac}}(A,B)$ We notice that $|A \setminus B| = |B \setminus A| = N_{\text{mut}}$, and $|A \cap B| = L - N_{\text{mut}}$. We note that the results in Theorem 3, Corollary 1 and Theorem 4 above still hold for a fixed N_{mut}. However, assuming a simple mutation model, N_{mut} is not a fixed quantity, rather a random variable Therefore, the analyses so far only connect $C_{\text{frac}}(A,B)$ to a fixed N_{mut}, as we have only considered the randomness from the FracMinHash sketching process so far. To quantify the impact of the mutation rate p on $C_{\text{frac}}(A,B)$, we now consider the randomness introduced by both the FracMinHash sketching process and the mutation process simultaneously.

Let $\mathcal{P} = (\Omega_1, \mathcal{F}_1, \mathbf{P}_1)$ and $\mathcal{S} = (\Omega_2, \mathcal{F}_2, \mathbf{P}_2)$ be the probability spaces corresponding to the mutation and FracMinHash sketching random processes, respectively. Here, $\Omega, \mathcal{F}$ and $\mathbf{P}$ denote the sample space, the sigma-algebra on the sample space, and the probability measure, respectively. We will use the subscript $\mathcal{P}, \mathcal{S}$ to indicate the product probability space, e.g. $\mathrm{E}_{\mathcal{P},\mathcal{S}}[\cdot]$ and $\mathrm{Var}_{\mathcal{P},\mathcal{S}}[\cdot]$. Hence we assume that the mutation process and the process of taking a FracMinHash sketch are independent. Before proceeding with the analysis, we make a note that the expectation and variance of N_{mut} under the simple mutation model with no spurious matches have been investigated in (Blanca et al 2022). As such, we already know $\mathrm{E}_{\mathcal{P}}[N_{\text{mut}}]$, $\mathrm{Var}_{\mathcal{P}}[N_{\text{mut}}]$ and $\mathrm{E}_{\mathcal{P}}[{N_{\text{mut}}}^2]$, and will use these results directly (see Blanca et al 2022, Table 1).

Theorem 5. *For $0 < s < 1$, if A and B are respectively distinct sets of k-mers of a sequence S and a sequence S' derived from S under the simple mutation model with mutation probability p such that $A \cap B$ is non-empty, then the expectation of $C_{frac}(A,B)$ in the product space $\mathcal{P}, \mathcal{S}$ is given by*

$$E_{\mathcal{P},\mathcal{S}}[C_{frac}(A,B)] = (1-p)^k, \tag{5}$$

where $\mathcal{P} = (\Omega_1, \mathcal{F}_1, \mathbf{P}_1)$ and $\mathcal{S} = (\Omega_2, \mathcal{F}_2, \mathbf{P}_2)$ are the probability spaces corresponding to the mutation and FracMinHash sketching random processes, respectively.

To demonstrate how the expected value of $C_{\text{frac}}(A,B)$ (considering both the random processes) react to the mutation rate p and the k-mer size k, we show $E_{\mathcal{P},\mathcal{S}}[C_{\text{frac}}(A,B)]$ in a heatmap in Figure 1. The heatmap shows that the expected value of the containment index decreases with a larger mutation rate and a larger k-mer size. This means that in the lighter cells (such as $k = 20$, $p = 0.001$), a small scale factor would suffice to find shared k-mers in two sketches – whereas in the darker cells (such as $k = 100$, $p = 0.1$), even a scale factor of 1.0 may not be sufficient because all k-mers are mutated. Consequently, a safe and meaningful choice of the scale factor s depends on the choices of p and k – which we discuss in more detail in later in this section.

Next, we turn to the more challenging task of calculating the variance of $C_{\text{frac}}(A,B)$ in the product space $\mathcal{P}, \mathcal{S}$.

Theorem 6. *For $0 < s < 1$, if A and B are respectively distinct sets of k-mers of a sequence S and a sequence S' derived from S under the simple mutation model with mutation probability p such that $A \cap B$ is non-empty, then the variance of $C_{frac}(A,B)$ in the product space $\mathcal{P}, \mathcal{S}$ is given by*

$$\underset{\mathcal{P},\mathcal{S}}{\mathrm{Var}}[C_{frac}(A,B)] = \frac{(1-s)}{sL^3\left(1-(1-s)^L\right)^2}(L\mathrm{E}_{\mathcal{P}}[N] - \mathrm{E}_{\mathcal{P}}[N^2]) + \frac{1}{L^2}\underset{\mathcal{P}}{\mathrm{Var}}(N_{mut}) \tag{6}$$

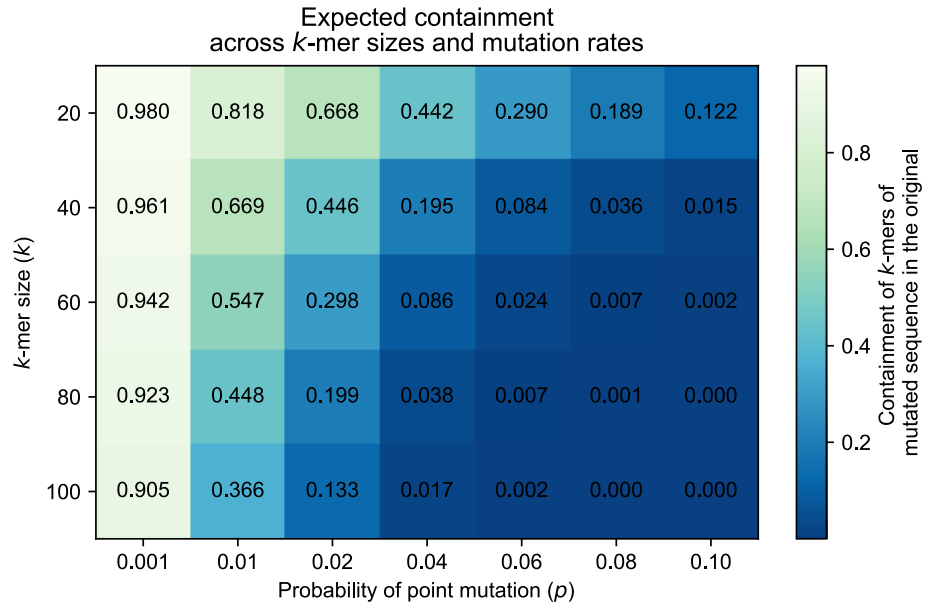

Fig. 1: $E_{\mathcal{P},\mathcal{S}}[C_{\text{frac}}(A,B)] = (1-p)^k$ across different mutation rates and k-mer sizes. Darker cells indicate a smaller value. The expected containment decreases with a larger mutation rate, and a larger k-mer size. This ideal case indicates that even a scale factor of $s = 1$ will be insufficient for large enough k sizes and p values.

where $\mathcal{P} = (\Omega_1, \mathcal{F}_1, \mathbf{P}_1)$ *and* $\mathcal{S} = (\Omega_2, \mathcal{F}_2, \mathbf{P}_2)$ *are the probability spaces corresponding to the mutation and FracMinHash sketching random processes, respectively.*

With the results of Theorem 5, we now have a point estimate of the mutation rate p given $C_{\text{frac}}(A,B)$, which is simply $p = 1 - C_{\text{frac}}(A,B)^{1/k}$. We next derive a hypothesis test for $C_{\text{frac}}(A,B)$ to capture the variability around the point estimate, and later turn it into a confidence interval.

Hypothesis test and confidence interval We observe that the marginal of $C_{\text{frac}}(A,B)$ with respect to the mutation process is simply $1 - \frac{N_{\text{mut}}}{L}$. Using the results in (Blanca et al 2022), we note that N_{mut} is asymptotically normally distributed when the mutation rate p and k-mer length k are independent of L, and L is sufficiently large. In Theorem 4, we showed that $C_{\text{frac}}(A,B)$ is normally distributed for a fixed N_{mut}. Therefore, considering the randomness from both the FracMinHash sketching and the mutation model independently, $C_{\text{frac}}(A,B)$ is asymptotically normal when all conditions are met. Using the statistics derived earlier, we obtain the following hypothesis test for $C_{\text{frac}}(A,B)$.

Theorem 7. *Let* $0 < s < 1$*, let* A *and* B *be two distinct sets of* k*-mers, respectively of a sequence* S *and a sequence* S' *derived from* S *under the simple mutation model with mutation probability* p*, such that* $A \cap B$ *is non-empty.*

Also, let $0 < \alpha < 1$*, and* C_{low} *and* C_{high} *be defined as follows.*

$$C_{low} = (1-p)^k - z_\alpha \sqrt{\frac{(1-s)}{sL^3\left(1-(1-s)^2\right)}\left(L\mathrm{E}_P[N_{mut}] - \mathrm{E}_P[{N_{mut}}^2]\right) + \frac{1}{L^2}\operatorname*{Var}_P(N_{mut})}$$

$$C_{high} = (1-p)^k + z_\alpha \sqrt{\frac{(1-s)}{sL^3\left(1-(1-s)^2\right)}\left(L\mathrm{E}_P[N_{mut}] - \mathrm{E}_P[{N_{mut}}^2]\right) + \frac{1}{L^2}\operatorname*{Var}_P(N_{mut})}.$$

Then, the following holds as $L \to \infty$ and when p and k are independent of L:

$$\Pr[C_{low} \leq C_{frac}(A, B) \leq C_{high}] = 1 - \alpha.$$

We can turn this hypothesis test into a confidence interval for the mutation rate p as follows.

Theorem 8. *Let A and B be two distinct sets of k-mers, respectively of a sequence S and a sequence S' derived from S under the simple mutation model with mutation rate p, such that $A \cap B$ is non-empty. Let $\mathrm{E}_{p_{fixed}}[X]$ and $\mathrm{Var}_{p_{fixed}}[X]$ denote the expectation and variance of a given random variable X under the randomness from the mutation process with fixed mutation rate p_{fixed}, respectively. Then, for fixed α, s, k and an observed $C_{frac}(A, B)$, there exists an L large enough such that there exist unique solutions $p = p_{low}$ and $p = p_{high}$ to the following equations, respectively,*

$$C_{frac}(A, B) = (1 - p_{low})^k + z_\alpha \sqrt{\frac{(1-s)}{sL^3\left(1-(1-s)^L\right)^2}\left(L\mathrm{E}_{p_{low}}[N_{mut}] - \mathrm{E}_{p_{low}}[{N_{mut}}^2]\right) + \frac{1}{L^2}\operatorname*{Var}_{p_{low}}(N_{mut})},$$

$$C_{frac}(A, B) = (1 - p_{high})^k - z_\alpha \sqrt{\frac{(1-s)}{sL^3\left(1-(1-s)^L\right)^2}\left(L\mathrm{E}_{p_{high}}[N_{mut}] - \mathrm{E}_{p_{high}}[{N_{mut}}^2]\right) + \frac{1}{L^2}\operatorname*{Var}_{p_{high}}(N_{mut})},$$

such that the following holds:

$$\lim_{L\to\infty} \Pr[p_{low} \leq p \leq p_{high}] = 1 - \alpha.$$

Setting parameters correctly: likelihood of pathological corner cases

In practice, one disadvantage of sketching techniques is that the size of the sketch (here controlled via the scale factor s) may be too small to distinguish between highly similar or dissimilar sequences. For example, given a small mutation rate p, one may need a very large scale factor, and so sketch, to be able to distinguish between a sequence and the mutated version. Similarly, if the mutation rate p is high and/or a large k size is used, it is possible that FracMinHash may report a containment value of 0, even though the true value is nonzero, yet small. These "corner cases" are precisely the ones where the confidence interval given by Theorem 8 will likely fail. One of these pathological cases shows up when there is nothing common between the two FracMinHash sketches $\mathbf{FRAC}_s(A)$ and $\mathbf{FRAC}_s(B)$. We observe that this occurs when $X_{A\cap B} = 0$. Now $X_{A\cap B}$ is distributed as a binomial distribution $\mathrm{Binom}(n, s)$ where $n = |A \cap B| = L - N_{\mathrm{mut}}$, so the probability of the intersection being empty with respect to the sketching process is:

$$\Pr_{\mathcal{S}}[X_{A\cap B} = 0] = (1 - s)^{L - N_{\mathrm{mut}}}.$$

Ideally, we would be able to directly calculate $\mathrm{E}_{\mathcal{P}}\left[\Pr_{\mathcal{S}}[X_{A\cap B} = 0]\right]$, the expected probability of this corner case happening. The challenge in doing so is that we do not have a closed form representation of the probability mass function (PMF) of N_{mut}. As a workaround, we developed a dynamic programming algorithm (presented in Section A.4) to compute $\Pr[N_{\mathrm{mut}} = x]$ given the parameters L and p.

Using this PMF, we can easily compute $\mathrm{E}_{\mathcal{P}}\left[\Pr_{\mathcal{S}}[X_{A\cap B} = 0]\right]$, which is the likelihood of the corner case that we observe nothing common between two sequences purely by chance. The remaining pathological case occurs when $p \neq 0$ and yet $\mathbf{FRAC}_s(A) = \mathbf{FRAC}_s(B)$ (i.e. the sketches are not large enough to distinguish between A and B). Similar to before, we have

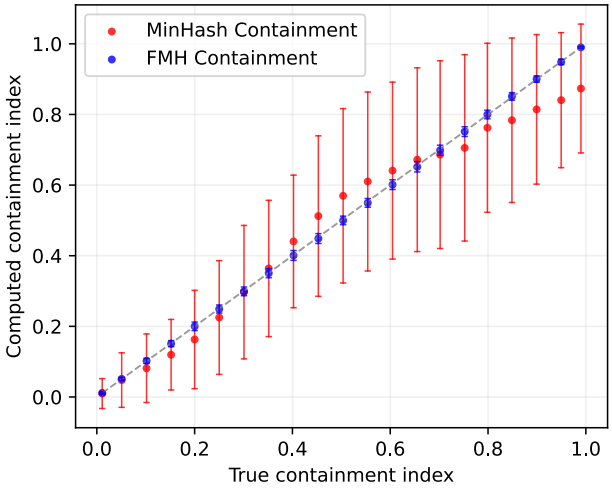

Fig. 2: True versus estimated containment index for both Mash and the FracMinHash approach for two sets with dissimilar sizes. The containment index of a *Staphylococcus* genome was computed when $C\%$ of this genome is inserted into an assembled metagenome. Error bars indicate standard deviation over hash seed values.

$$\Pr_{\mathcal{S}}\left[X_{A\setminus B}=0, X_{B\setminus A}=0\right] = \Pr_{\mathcal{S}}\left[X_{A\setminus B}=0\right]\Pr_{\mathcal{S}}\left[X_{B\setminus A}=0\right] = (1-s)^{2N_{\text{mut}}},$$

and hence, by calculating $\mathrm{E}_{\mathcal{P}}\left[(1-s)^{2N_{\text{mut}}}\right]$ using the PMF of N_{mut}, we can obtain the likelihood of the latter pathological case. Here, $A \setminus B$ and $B \setminus A$ are disjoint sets, allowing us to use the independence of $X_{A\setminus B}$ and $X_{B\setminus A}$. We assume both $A \setminus B$ and $B \setminus A$ are non-empty.

It is important to note the importance to characterize these "corner cases" as without it, a user would be unable to determine if the observed containment index of, say, zero is due to the sequences under consideration being highly diverged, or else the scale factor chosen is much too small. into sourmash (Brown and Irber 2016) for precisely this purpose – to help practitioners assess if containment estimates of 0 or 1 are due to parameter settings (eg. scale value too high/low), or else are biologically meaningful.

Results

FracMinHash accurately estimates containment index for sets of very different sizes

We first show that FracMinHash can estimate the true containment index better than MinHash when the sizes of two sets are dissimilar. For this experiment, we compared FracMinHash with the popular MinHash implementation tool Mash (Ondov et al 2016). We took a *Staphylococcus* genome from the GAGE dataset (Salzberg et al 2012) and selected a subsequence that covers $C\%$ of the whole genome in terms of number of bases, added this sequence to a metagenome, and calculated the containment of *Staphylococcus* in this "super metagenome." The metagenome we used is a WGS metagenome sample consisting of approximately 1.3G bases. We used a scale factor of 0.005 for FracMinHash, and we set the number of hash functions for Mash at 4000, since Mash works reasonably well with even only 1000 hash functions to find the containment of *Staphylococcus* genome in the unaltered metagenome. We picked 0.005 because it generates small enough sketch sizes to be computationally inexpensive, and at the same time ensures that the likelihoods of the corner cases are minimal.

	$L = 10$ K			$L = 100$ K			$L = 1$ M		
$p = 0.001$		0.1	0.2	0.001	0.1	0.2	0.001	0.1	0.2
$k = 21$	95.7	94.9	95.0	95.2	95.0	95.3	95.0	94.8	95.1
$k = 51$	95.2	94.6	N/A	95.2	95.5	N/A	95.0	94.8	N/A
$k = 100$	95.1	N/A	N/A	95.2	N/A	N/A	95.1	94.7	N/A

Table 1: The percentage of experiments that resulted in the true mutation rate falling within the 95% confidence interval given in Theorem 8 when using various mutation rates across multiple k-mer sizes and L values. A scale factor of $s = 0.1$ was used. The results show an average over 10,000 simulations for each setting. N/A entries indicate that the parameters are not particularly meaningful and will not produce interpretable results, either because $E[N_{\text{mut}}] \approx L$ in these cases (almost all k-mers are mutated), or because the scale factor is too small to differentiate between the two FracMinHash sketches. These results show that the confidence interval presented in Theorem 8 is statistically significant for meaningful parameter settings. These results reveal that k-mers are highly sensitive to mutation rates, and practitioners may need to use shorter k-mer lengths to distinguish highly dissimilar sequences.

We repeated this setup for different values of C, and compared the containment index calculated by Mash and FracMinHash in Figure 2. We show the mean values for multiple runs with different seeds in the figure, and use the error bars to show the standard deviation. Mash primarily reports MinHash Jaccard index, so we converted the Jaccard into containment by counting the number of distinct k-mers using brute force.

Figure 2 illustrates that while Mash and FracMinHash both faithfully estimate the true containment index, the FracMinHash approach more accurately estimates the containment index as this index increases in value. In addition, the estimate is more precise as demonstrated by the size of the error bars on the estimates. This is likely due to the fact that while Mash and FracMinHash both use a sketch of size 4,000 for the *Staphylococcus* genome, Mash uses the same fixed value of 4,000 when forming a sketch for the metagenome, while FracMinHash selects a sketch size that scales with the size of the metagenome. This can be seen most starkly when the metagenome is significantly larger than the query genome.

FracMinHash gives accurate confidence intervals around mutation rates

Next, we show that the confidence interval from Theorem 8 for the mutation rate p is statistically sound and works well in practice. To do so, we performed 10,000 simulations of sequences of length $L = 10$k, 100k and 1M that underwent the simple mutation model with $p = 0.001$, 0.1 and 0.2. We then used a scale factor of $s = 0.1$ when calculating p_{low} and p_{high} for a 95% confidence interval and repeated this for k-mer sizes of 21, 51 and 100. Table 1 records the percentage of experiments that resulted in $p_{\text{low}} \leq p \leq p_{\text{high}}$ and demonstrates that the confidence intervals indeed are approximately 95%. Results with other scale factors are presented in Tables S1 and S2.

In some of these settings (indicated with N/A) shown in Table 1, we skipped the experiment because these do not yield a meaningful result. Mostly, like the darkest cells in Figure 1, these are cases where all or almost all k-mers are mutated and consequently, we observe a zero containment, leading to undefined results. In the other cases, the number of shared k-mers is too small to use a scale factor of 0.1 and finding a representative number of shared k-mers in the FracMinHash sketch – again – resulting in a zero containment. To better understand these settings, we listed the expected number of non-mutated k-mers (studied in (Blanca et al 2022)) in Table S3 – only a 10% of which is expected to end up in the sketch, which explains the N/A entries in Table 1.

FracMinHash more accurately estimates mutation distance

On simulated data We finally compare the Mash estimate and FracMinHash estimate (given as a confidence interval) of mutation rates. For this experiment, we simulated point mutations in the aforementioned *Staphylococcus* genome at a mutation rate p, and then calculated the distance of the original *Staphylococcus* genome with this mutated genome using both Mash and the interval given by Theorem 9. The results are shown in Figure 3a. This plot shows that Mash overestimates the mutation rate by a noticeable degree, with increasing inaccuracy as the mutation distance increases. This is likely due to the Mash distance assuming a Poisson model for how mutations affect k-mer occurrences, which has been shown to be violated when considering a point mutation model. In contrast, the point estimate given by Theorem 9 is fairly close to the true mutation rate, and the confidence interval accurately entails the true mutation rate.

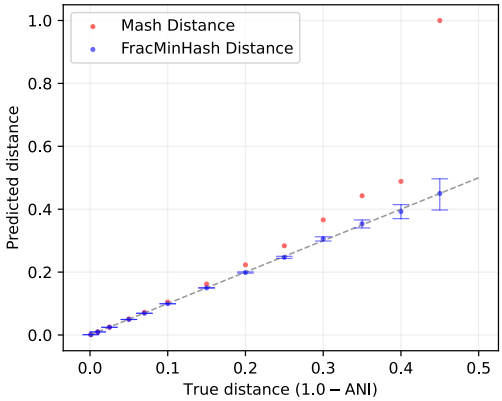

(a) Estimates of evolutionary distances between original and mutated *Staphylococcus* genome

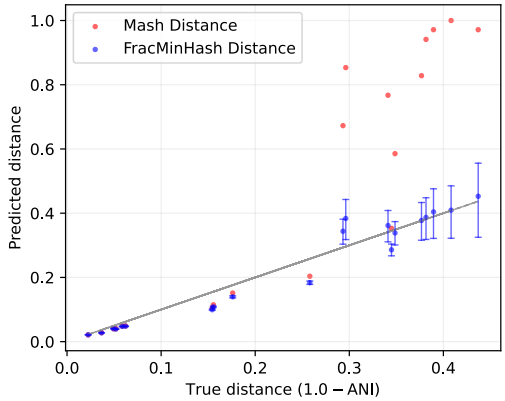

(b) Estimates of evolutionary distances between pairs of real bacterial genomes

Fig. 3: Mash distances and FracMinHash estimates of evolutionary distance (given in terms of one minus the average nucleotide identity: ANI) when (a) introducing point mutations to a *Staphylococcus* genome at a known rate, and (b) between pairs of real bacterial genomes. Error bars indicate the confidence intervals surrounding the FracMinHash estimate calculated using Theorem 8. To obtain the FracMinHash estimates, k-mer size $k = 21$ and scale factor $s = 0.1$ was used.

On real data We next present pairwise mutation distances between a collection of real genomes using both Mash and the interval in Theorem 8. To make a meaningful comparison, it is important to compute the true mutation distance (or equivalently, the average nucleotide identity) between a pair of genomes. For this purpose, we used OrthoANI (Lee et al 2016), a fast ANI calculation tool. From amongst 199K bacterial genomes downloaded from NCBI, we randomly filtered out pairs of genomes so that the pairwise ANI ranges from 0.5 to 1. For visual clarity, we kept at most 3 pairs of genomes for any ANI interval of width 5%. We used 4000 hash functions to run Mash, and set $L = (|A| + |B|)/2$ for the confidence intervals in Theorem 9, where $|A|$ and $|B|$ denote the numbers of distinct k-mers in the two genomes in a pair. The results are presented in Figure 3b.

Clearly, Mash overestimates the mutation distance, particularly for moderate to high distances. In contrast, the confidence intervals given by Theorem 8 perform significantly better. It is noticeable that the confidence intervals are not as accurate as in the case of a simulated genome (presented in Figure 3a). This is natural because in this real setup, the sizes of the genomes are very dissimilar,

have repeats, and very easily violate the simplifying assumptions of the simple mutation model. Nonetheless, these results demonstrate the usefulness of the proposed approach even when the model assumptions are violated.

We conclude this section by computing ANI using FracMinHash sketches ($k = 21$, $s = 0.1$) and a few other well-known tools – namely, Mash (Ondov et al 2016), `pyani` (Pritchard et al 2016), and `fastani` (Jain et al 2018). To build the set of genomes for this experiment, we first selected representative genomes from ten species with the largest number of genomes in GTDB-rs207 (7 bacteria and 3 archaea) (Parks et al 2022). Then, we built an "evolutionary path" for each of these "anchor" genomes by selecting three non-representative genomes sharing each taxonomic rank, e.g. three genomes in the same genus but different species, three in the same family but different genus, etc. We computed pairwise ANI from the "anchor" representative genome to each of these genomes using all methods. Using this approach allows usage of real genomes across a range of ANI values. The results are shown in Figure 4. Like the previous set of figures, we again plotted the ANI computed using OrthoANI (Lee et al 2016) on the x-axis.

As above, Mash cannot reliably differentiate genomes at ANI below 70%. In addition, as most ANI tools are recommended for use only above 75-80% ANI, the lack of meaningful ANI values below 75% for `fastani` is expected. In the 80-100% range, all tools correlate well with OrthoANI (shown in dashed grey), with least-squares fits for FracMinHash and `pyani` in blue and green, respectively. However, both `pyani` and FracMinHash both correlate with OrthoANI quite well even below 80% ANI, with FracMinHash performing slightly better in this low range. From 60-80% ANI, FracMinHash had a Pearson correlation coefficient with OrthoANI of 0.79 while `pyani` had a correlation of 0.69 with OrthoANI.

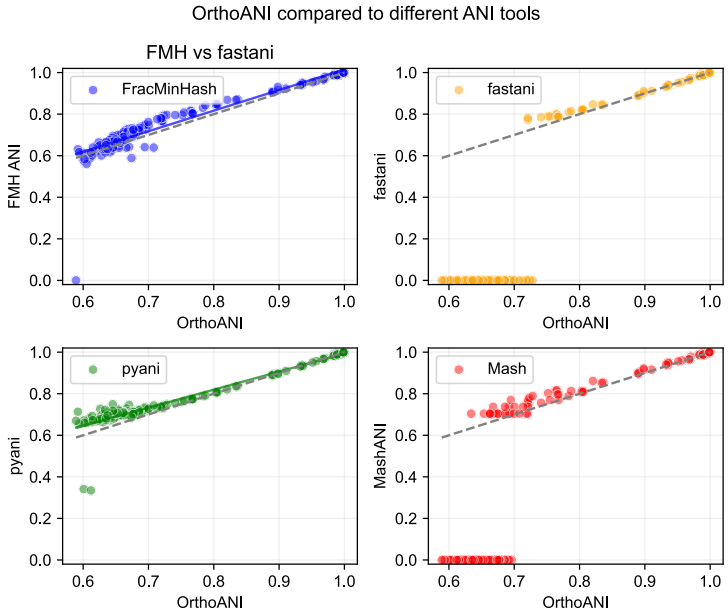

Fig. 4: Pairwise ANI estimation among a selection of genomes from the GTDB database. The dashed line represents ANI computed using OrthoANI. The solid blue and green lines show the least-squares fit for the ANI scores computed using FracMinHash and `pyani`, respectively. Mash and `fastani` both have many zero-ed out values, and therefore, the least-squares fit is not shown for these two.

Discussion

In contrast to classic MinHash, which uses a fixed sketch size, FracMinHash automatically scales the size of the sketch based on the size of the input data. This has the advantage of facilitating accurate comparison of sets of very different sizes, extending sketch-based comparisons to metagenomic datasets, including streaming-based analyses and large-scale database searches. Given that a user has control over what percentage of the data to keep in the sketch (in terms of s), reasonable estimates can be made about sketch sizes *a priori*, and trade-offs can be employed to prevent large sketch sizes while maintaining sufficient resolution for search. One particularly attractive feature of FracMinHash is its analytical tractability: as we have demonstrated, it is relatively straightforward to characterize the performance of FracMinHash, derive its statistics, and study how it interacts with a simple mutation model. Given these advantages, it seems reasonable to favor FracMinHash in situations where sets of differing sizes are being compared, or else when fast and accurate estimates of mutation rates are desired (particularly for moderate to high mutation rates). We believe that using FracMinHash can enable fast metagenomic binning by discarding genomes irrelevant to a metagenomic sample (based on low containment scores), let users filter genomes from a reference database using ANI thresholds, allow practitioners to use the confidence intervals with taxonomic tree and sample bootstrap phylogenies off of the taxonomy – and realize many other useful applications.

This manuscript focuses on theoretical analyses using the containment index – primarily because deriving confidence intervals around the mutation rate from the Jaccard index proved to be mathematically intractable. We still showed how to obtain a point estimate of the mutation rate using an observed Jaccard index. These analyses are included in the supplemental materials: theoretical analysis (Section A.7), derivation of a point estimate of mutation rate (and ANI) using the Jaccard index (Section A.8), and results on the utility of this point estimate (Figure S1).

Software availability

A Python-based implementation of the algorithms and theorems we derive is freely available at https://github.com/KoslickiLab/mutation-rate-ci-calculator. The results presented in this paper can be reproduced using the code at https://github.com/KoslickiLab/FracMinHash-reproducibles. All code in these github repositories are also available as supplemental materials.

Competing interest statement

The authors declare no competing interests.

Acknowledgements

MR and DK were supported by NSF award No. DMS-2029170 and the NIH grant 1R01GM146462. NP was supported by NSF grants 1711984 and 2018911. The authors express their sincere thanks to Luiz Irber and Paul Medvedev for their invaluable inputs to this manuscript.

Author contributions: DK and MR developed the theoretical results with input from NTP for biological application. MR prepared all the results except for the last figure, the results of which were prepared by NTP. DK and MR wrote the theorems and proofs. MR prepared all plots and the manuscript. All authors reviewed and curated the manuscript.

References

Agresti, A. 2012. *Categorical data analysis*. Vol. 792. John Wiley & Sons.

Birol, I., Jackman, S. D., Nielsen, C. B., Qian, J. Q., Varhol, R., Stazyk, G., Morin, R. D., Zhao, Y., Hirst, M., Schein, J. E., et al. 2009. De novo transcriptome assembly with abyss. *Bioinformatics*, *25*. 21., 2872–2877.

Blanca, A., Harris, R. S., Koslicki, D., & Medvedev, P. 2022. The statistics of k-mers from a sequence undergoing a simple mutation process without spurious matches. *Journal of Computational Biology*, *29*. 2., 155–168.

Bloom, B. H. 1970. Space/time trade-offs in hash coding with allowable errors. *Communications of the ACM*, *13*. 7., 422–426.

Breitwieser, F. P., Baker, D., & Salzberg, S. L. 2018. Krakenuniq: Confident and fast metagenomics classification using unique k-mer counts. *Genome biology*, *19*. 1., 1–10.

Broder, A. Z. 1997. On the resemblance and containment of documents. *Proceedings. Compression and Complexity of SEQUENCES 1997 (Cat. No. 97TB100171)*, 21–29.

Brown, C. T., & Irber, L. 2016. Sourmash: A library for minhash sketching of dna. *Journal of Open Source Software*, *1*. 5., 27.

Chin, C.-S., & Khalak, A. 2019. Human genome assembly in 100 minutes. *bioRxiv*, 705616. https://doi.org/10.1101/705616

Crusoe, M. R., Alameldin, H. F., Awad, S., Boucher, E., Caldwell, A., Cartwright, R., Charbonneau, A., Constantinides, B., Edvenson, G., Fay, S., et al. 2015. The khmer software package: Enabling efficient nucleotide sequence analysis. *F1000Research*, *4*.

Ekim, B., Berger, B., & Chikhi, R. 2021. Minimizer-space de bruijn graphs: Whole-genome assembly of long reads in minutes on a personal computer. *Cell Systems*.

Flajolet, P., Fusy, É., Gandouet, O., & Meunier, F. 2007. Hyperloglog: The analysis of a near-optimal cardinality estimation algorithm. *Discrete Mathematics and Theoretical Computer Science*, 137–156.

Ghosh, P., & Kalyanaraman, A. 2017. Fastetch: A fast sketch-based assembler for genomes. *IEEE/ACM transactions on computational biology and bioinformatics*, *16*. 4., 1091–1106.

Irber, L. C., Brooks, P. T., Reiter, T. E., Pierce-Ward, N. T., Hera, M. R., Koslicki, D., & Brown, C. T. 2022. Lightweight compositional analysis of metagenomes with fracminhash and minimum metagenome covers. *bioRxiv*. https://doi.org/10.1101/2022.01.11.475838

Irber Jr, L. C. 2020. *Decentralizing indices for genomic data*. Doctoral dissertation. University of California, Davis.

Jain, C., Rodriguez-R, L. M., Phillippy, A. M., Konstantinidis, K. T., & Aluru, S. 2018. High throughput ani analysis of 90k prokaryotic genomes reveals clear species boundaries. *Nature communications*, *9*. 1., 1–8.

Koslicki, D., & Zabeti, H. 2019. Improving minhash via the containment index with applications to metagenomic analysis. *Applied Mathematics and Computation*, *354*, 206–215.

LaPierre, N., Alser, M., Eskin, E., Koslicki, D., & Mangul, S. 2020. Metalign: Efficient alignment-based metagenomic profiling via containment min hash. *Genome biology*, *21*. 1., 1–15.

LaPierre, N., Mangul, S., Alser, M., Mandric, I., Wu, N. C., Koslicki, D., & Eskin, E. 2019. Micop: Microbial community profiling method for detecting viral and fungal organisms in metagenomic samples. *BMC genomics*, *20*. 5., 1–10.

Lee, I., Kim, Y. O., Park, S.-C., & Chun, J. 2016. Orthoani: An improved algorithm and software for calculating average nucleotide identity. *International journal of systematic and evolutionary microbiology*, *66*. 2., 1100–1103.

Li, H. 2018. Minimap2: Pairwise alignment for nucleotide sequences. *Bioinformatics*, *34*. 18., 3094–3100.

Miclotte, G., Heydari, M., Demeester, P., Audenaert, P., & Fostier, J. 2015. Jabba: Hybrid error correction for long sequencing reads using maximal exact matches. *International Workshop on Algorithms in Bioinformatics*, 175–188.

Ondov, B. D., Treangen, T. J., Melsted, P., Mallonee, A. B., Bergman, N. H., Koren, S., & Phillippy, A. M. 2016. Mash: Fast genome and metagenome distance estimation using minhash. *Genome biology*, *17*. 1., 1–14.

Parks, D. H., Chuvochina, M., Rinke, C., Mussig, A. J., Chaumeil, P.-A., & Hugenholtz, P. 2022. Gtdb: An ongoing census of bacterial and archaeal diversity through a phylogenetically consistent, rank normalized and complete genome-based taxonomy. *Nucleic acids research*, *50*. D1., D785–D794.

Pierce, N. T., Irber, L., Reiter, T., Brooks, P., & Brown, C. T. 2019. Large-scale sequence comparisons with sourmash. *F1000Research*, *8*.

Pritchard, L., Glover, R. H., Humphris, S., Elphinstone, J. G., & Toth, I. K. 2016. Genomics and taxonomy in diagnostics for food security: Soft-rotting enterobacterial plant pathogens. *Analytical Methods*, *8*. 1., 12–24.

Sahlin, K., & Medvedev, P. 2021. Error correction enables use of oxford nanopore technology for reference-free transcriptome analysis. *Nature Communications*, *12*. 1., 1–13.

Salzberg, S. L., Phillippy, A. M., Zimin, A., Puiu, D., Magoc, T., Koren, S., Treangen, T. J., Schatz, M. C., Delcher, A. L., Roberts, M., et al. 2012. Gage: A critical evaluation of genome assemblies and assembly algorithms. *Genome research*, *22*. 3., 557–567.

Sueoka, N. 1995. Intrastrand parity rules of dna base composition and usage biases of synonymous codons. *Journal of molecular evolution*, *40*. 3., 318–325.

Takahata, N., & Kimura, M. 1981. A model of evolutionary base substitutions and its application with special reference to rapid change of pseudogenes. *Genetics*, *98*. 3., 641–657.

Tavaré, S. 1984. Line-of-descent and genealogical processes, and their applications in population genetics models. *Theoretical population biology*, *26*. 2., 119–164.

Viehweger, A., Blumenscheit, C., Lippmann, N., Wyres, K. L., Brandt, C., Hans, J. B., Hölzer, M., Irber, L., Gatermann, S., Lübbert, C., et al. 2021. Context-aware genomic surveillance reveals hidden transmission of a carbapenemase-producing klebsiella pneumoniae. *Microbial genomics*, *7*. 12.

Zhang, Q., Pell, J., Canino-Koning, R., Howe, A. C., & Brown, C. T. 2014. These are not the k-mers you are looking for: Efficient online k-mer counting using a probabilistic data structure. *PloS one*, *9*. 7., e101271.